

## CHAPTER III

### THEORY AND CONCEPT

This chapter presents the theory and concept related to well test and wireline formation test. Pressure transient analysis (PTA) is used as a method to obtain reservoir parameters.

#### 3.1 Well Test and Wireline Formation Test Interpretation

Well test is a process to monitor the response of the reservoir to changing production or injection. The characteristic of response can infer the reservoir properties. Therefore, well test interpretation is an inverse problem in that model parameters can be inferred by analyzing model response to a given input as shown in Figure 3.1

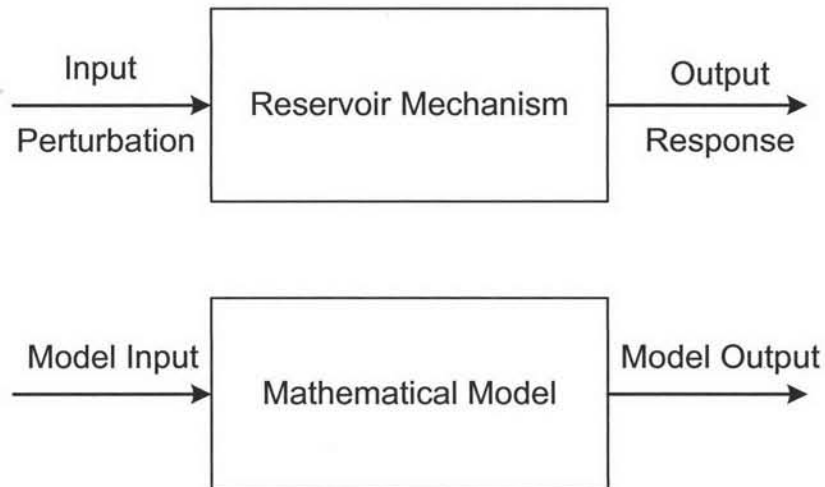


Figure 3.1: Inverse problem (Horne, 1995).

Since the response measured in a well test is a pressure response, well test analysis is sometime called pressure transient analysis (PTA).

Since the break-through of wireline formation test in oil and gas business and its promising development in pressure response measurement, wireline formation test is now become an alternative method to obtain reservoir parameters. It uses the same principal as advanced well test analysis to interpret information from pressure response data.

## 3.2 Pressure Transient Analysis (PTA)

### 3.2.1 Well Test Concept

From conservation of mass, an equation can be written for an elementary volume as

$$\text{Mass In} - \text{Mass Out} = \text{Increase In Storage} \quad (3.1)$$

After balancing the mass and using Darcy's law to describe the flow of fluid in porous media, the well-known diffusivity equation is

$$\nabla^2 p = \frac{\phi \mu c_t}{k} \frac{\partial p}{\partial t} \quad (3.2)$$

where

$p$  = pressure

$\phi$  = porosity

$\mu$  = fluid viscosity

$c_t$  = total compressibility

$k$  = formation permeability

$t$  = time

### 3.2.2 Wireline Formation Test Concept

As previously mentioned that wireline formation test uses the same concept as advanced well test analysis, thus diffusion equation was solved to meet the specify initial condition and boundary.

To analyze pressure response within the formation, three different types of flow regimes are considered. These are linear, radial and spherical flow. As described earlier, Moran and Finklea (1962) showed that in a Wireline formation test the last two, radial and spherical flow regimes, are present. In addition, they proposed an equation for spherical flow.

For spherical Flow, Moran and Finklea (1962) developed the equation

$$p(t) = p_i - \frac{\mu}{4\pi k} \sqrt{\frac{\alpha}{\pi}} \frac{V}{t} \left[ \frac{1}{\sqrt{\Delta t}} - \frac{1}{\sqrt{t + \Delta t}} \right] \quad (3.3)$$

For radial flow, Horner (1951) derived the equation for buildup period

$$p(t) = p_i - \frac{\mu}{4\pi k h} \frac{V}{t} [\ln(t + \Delta t) - \ln \Delta t] \quad (3.4)$$

Where

- $\mu$  = fluid viscosity (poises)
- $k$  = formation permeability (cm<sup>2</sup>)
- $\alpha$  =  $\mu c \phi / k$  (sec/cm<sup>2</sup>)
- $c$  = compressibility (cm<sup>2</sup>/dyne)
- $V$  = total volume of fluid produced (cm<sup>2</sup>)
- $t$  = total time the tool is opened (sec)
- $\Delta t$  = time after the tool is closed (sec) (time for buildup)
- $p_i$  = initial reservoir pressure (dynes/cm<sup>2</sup>)
- $p(t)$  = pressure at any time  $t$  (dynes/cm<sup>2</sup>)
- $A$  = cross-sectional area (cm<sup>2</sup>)
- $h$  = bed thickness of interval tested (cm)

In this study, the equation for spherical flow is as follows :

$$\Delta p = \frac{q B \mu}{2 a_1 k_{xyz} r_s} \left[ 1 - \sqrt{\frac{\phi \mu c_t r_s^2}{\pi a_2 k_{xyz}} \frac{1}{\sqrt{\Delta t}}} + S_p \right] \quad (3.5)$$

The spherical permeability is

$$k_{xyz} = \sqrt[3]{k_x k_y k_z} = \sqrt[3]{k_{xy}^2 k_z} \quad (3.6)$$

And, the horizontal permeability is

$$k_{xy} = \sqrt{k_x k_y} \quad (3.7)$$

where

- $\mu$  = fluid viscosity (cp)
- $\phi$  = porosity (fraction)
- $k_{xyz}$  = spherical permeability (mD)
- $k_{xz}$  = horizontal permeability (mD)
- $k_z$  = vertical permeability (mD)
- $c_t$  = total compressibility (psi<sup>-1</sup>)
- $B$  = formation volume factor (RB/STB)
- $\Delta t$  = time (hrs)
- $p_i$  = initial reservoir pressure (psi)
- $\Delta p$  = pressure drop (psi)
- $q$  = flowrate ( STB/Day)
- $r_s$  = probe radius (ft)
- $S_p$  = probe skin factor
- $a_1$  = 0.00708
- $a_2$  = 0.0002637

### 3.3 Radius of Investigation

During the test, the pressure response follows a diffusion type of response. Practically there will be some distance from the well at which the pressure change is so small to be undetectable. It can be referred this point as radius of investigation. Since the definition of radius of investigation depends on the definition of detectable pressure response, several definitions of radius of investigation equation have been proposed.

The most common use is Lee's definition. The radius of investigation is defined as the point where the pressure change is maximum.

$$r_{inv} = 0.032 \sqrt{\frac{kt}{\phi \mu c_t}} \quad (3.8)$$

where

- $\mu$  = fluid viscosity (cp)
- $\phi$  = porosity (fraction)
- $k$  = permeability (mD)
- $c_t$  = total compressibility ( $\text{psi}^{-1}$ )
- $t$  = drawdown time (hrs)

To evaluate the permeability from wireline formation test data, radius of investigation is taken into account to observe the approximate distance the pressure responds in reservoir. This is to appraise how far permeability calculated from WFT data can represent.

### 3.4 Type Curve for Wireline Formation Test

Figure 3.2 is the type curve representation of the model for wireline formation test when both upper and lower boundaries are infinite. The two flow regimes are wellbore storage defined by a unit slope and spherical flow defined by a negative half slope as shown in the figure.

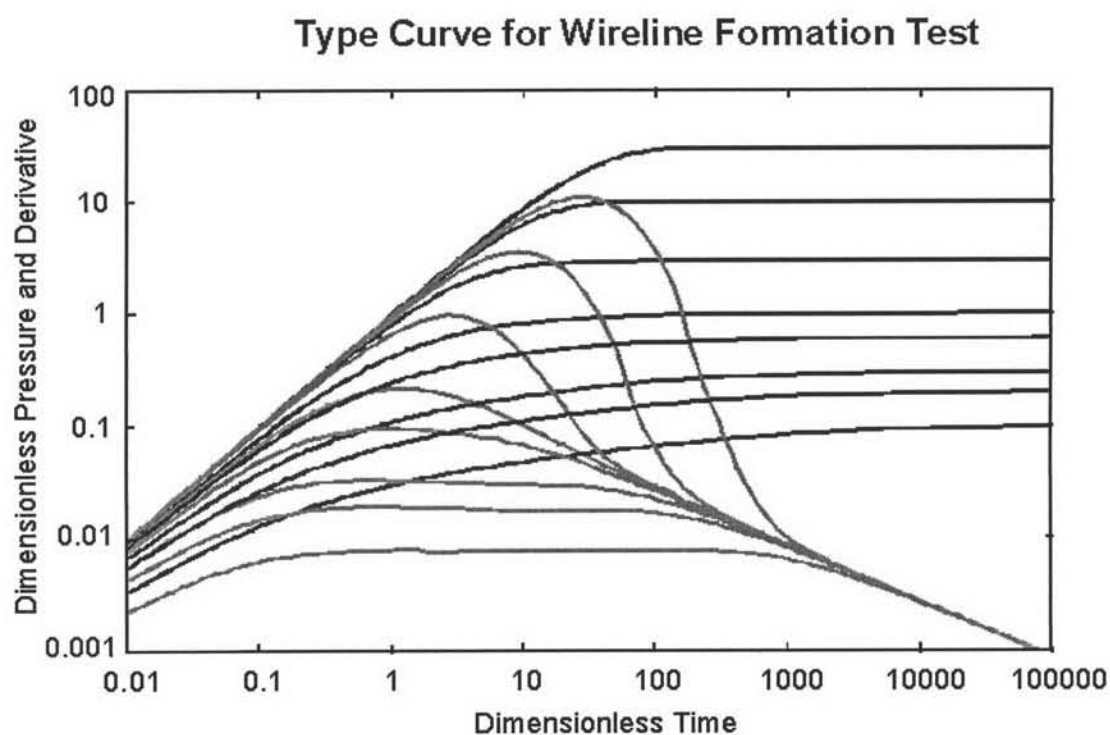


Figure 3.2: Type curve for wireline formation test.

### 3.5 Flow Regime

There are three flow regimes involving in this study.

#### 3.5.1 Spherical Flow

When the fluid in the formation is moving into the probe, which has a small diameter, the flow regime is spherical as shown in Figure 3.3. In a pressure derivative

log-log plot as in Figure 3.4, at early time, the pressure response is influenced by wellbore storage. Then, spherical flow occurs and can be identified by a straight line with a negative half slope. The spherical permeability ( $k_{xyz}$ ) can be obtained from this flow regime.

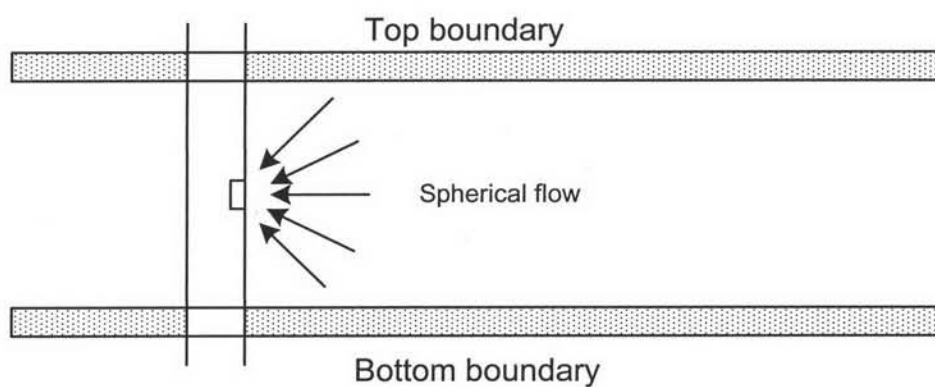


Figure 3.3: Schematic of spherical flow.

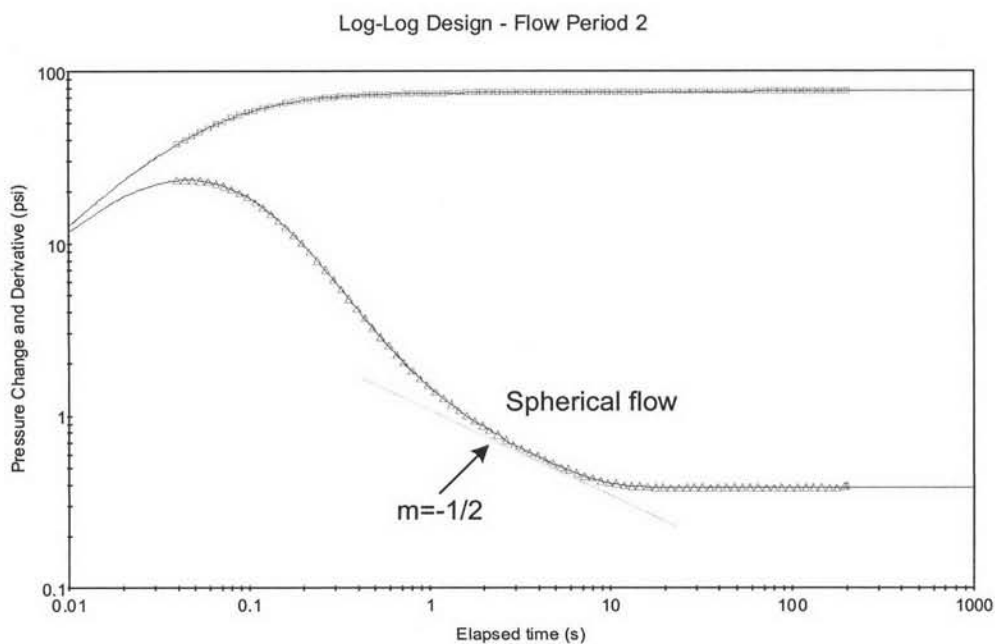


Figure 3.4: Pressure change and pressure derivative of spherical flow.

### 3.5.2 Radial Flow

When the fluid flows in the formation and encounters upper and lower boundaries as shown in Figure 3.5, the flow regime is now radial or cylindrical flow. Vertical to horizontal permeability ratio can be calculated if the upper and lower boundaries are known from other source of data such as well logging. In a pressure derivative log-log plot as in Figure 3.6, at early times, the pressure response is influenced by wellbore storage. After that, spherical flow occurs, and then radial flow developed as pressure response reaches the top and bottom boundaries and can be identified by horizontal line of pressure derivative. The horizontal permeability ( $k_{xy}$ ), vertical permeability ( $k_z$ ), and vertical to horizontal permeability ratio ( $k_z / k_{xy}$ ) can be obtained from this flow regime.

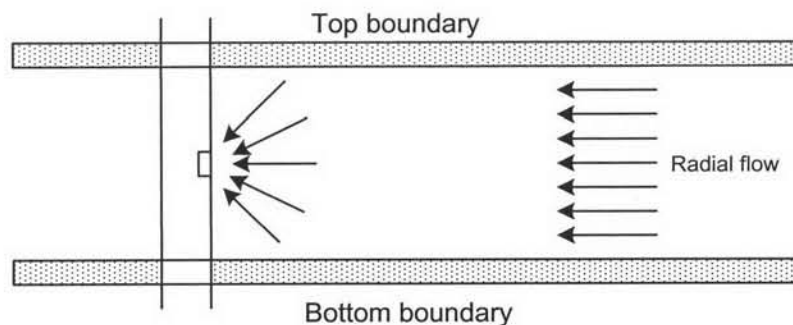


Figure 3.5: Schematic of radial flow.



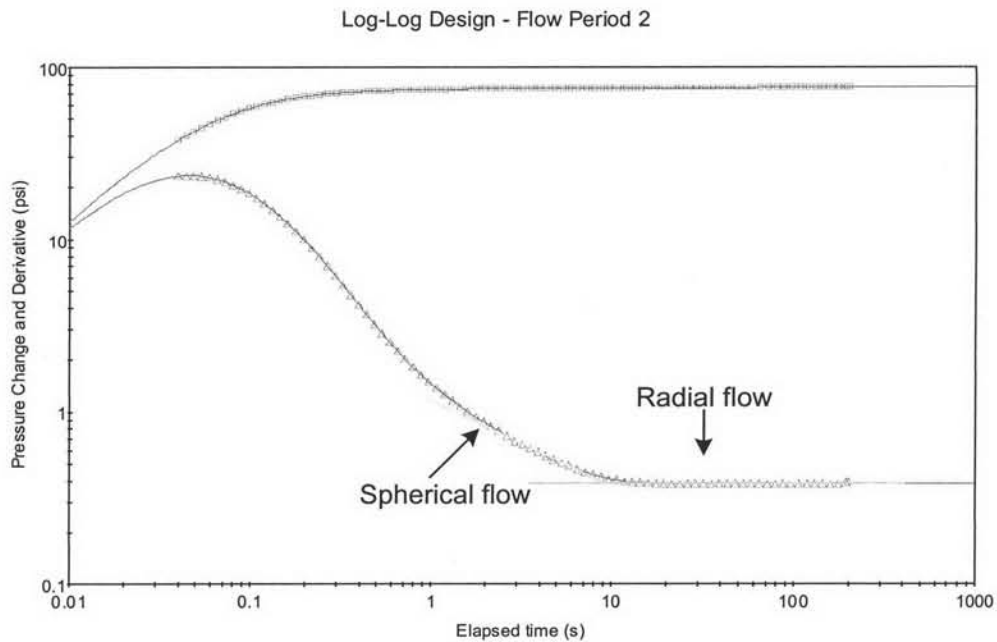


Figure 3.6: Pressure change and pressure derivative of radial flow.

### 3.5.3 Hemispherical Flow

When the probe was placed close to the top or bottom boundary, spherical flow will not fully developed. Some of the pressure response hits the closer boundary and start to develop into radial flow while the others still acts like spherical flow as shown in Figure 3.7. In a pressure derivative log-log plot as shown in Figure 3.8, at early time, the pressure response is influenced by wellbore storage, and then spherical flow occurs. After that, as the probe is placed near top or bottom boundary, hemispherical flow takes place, identified by another negative half slope in a derivative plot. When the pressure response reaches both the top and bottom boundaries, radial flow is then fully developed.

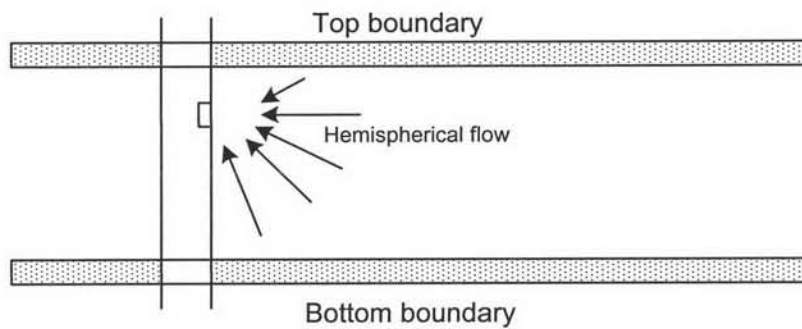


Figure 3.7: Schematic of hemispherical flow.

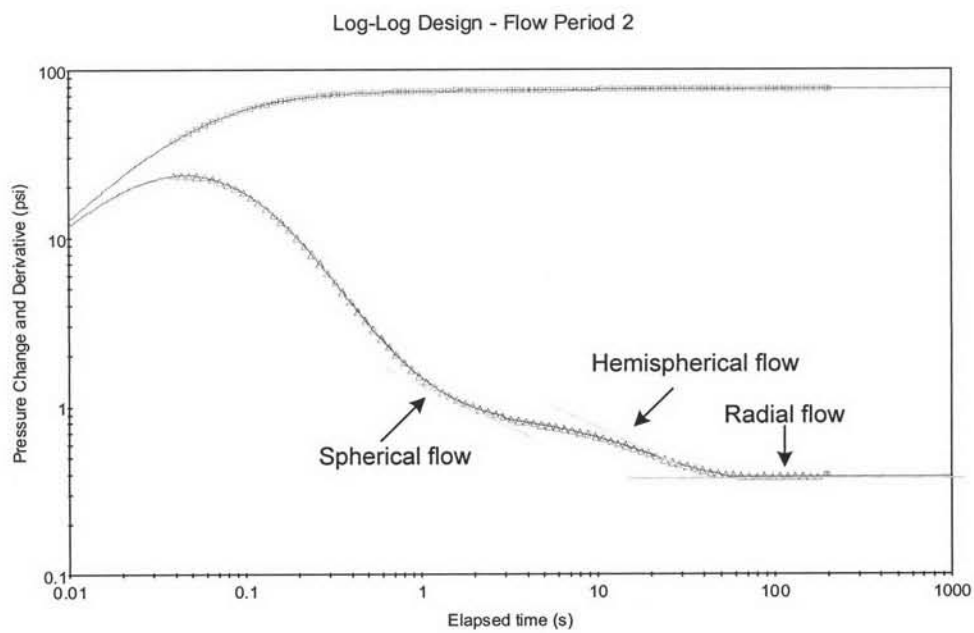


Figure 3.8: Pressure change and pressure derivative of hemispherical flow.

## 3.6 Multilayer Reservoir

Some reservoirs consist of stratified formations. There are two types of reservoir layering, depending on the pressure communication with each other within the same reservoir.

### 3.6.1 Commingled System

The layers are hydraulically separated within the formation and communicate only through the wellbore as shown in Figure 3.9.

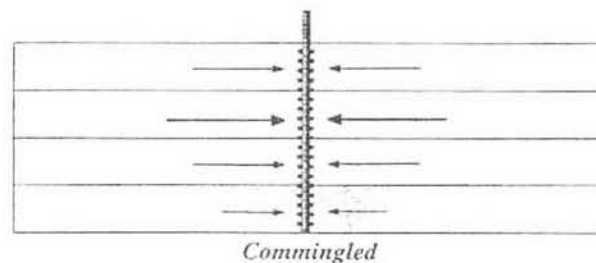


Figure 3.9: Commingled system (Horne, 1995).

### 3.6.2 Crossflow System

The layers are in hydraulic communication within the formation. There is formation crossflow between layers as shown in Figure 3.10.

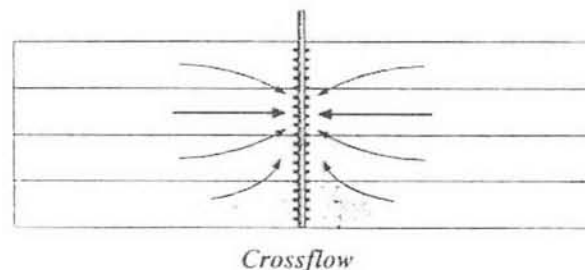


Figure 3.10: Crossflow system (Horne, 1995).

In this study, formation with multilayer system with formation crossflow is considered.

### 3.7 Averaging Techniques

There are three types of averaging technique used in this study to compare the calculated averaging permeability of multilayer system with permeability obtained from interpretation using a well test interpretation software.

#### 3.7.1 Arithmetic Mean

The arithmetic mean of a set of values is the quantity commonly called the mean or the average.

Given a set of samples,

$$X = \{x_1, x_2, \dots, x_n\} \quad (3.9)$$

and corresponding non-negative weight,

$$W = \{w_1, w_2, \dots, w_n\} \quad (3.10)$$

the arithmetic mean is

$$\bar{x} = \frac{\sum_{i=1}^n x_i w_i}{\sum_{i=1}^n w_i} \quad (3.11)$$

where

- $\bar{x}$  = arithmetic mean
- $x_i$  = values of samples  $i$
- $n$  = number of samples
- $w_i$  = weight of sample  $i$

### 3.7.2 Geometric Mean

The geometric mean of a sequence from Equation (3.9) and (3.10) is the number  $G$  defined by

$$G = \left( \prod_{i=1}^n x_i^{w_i} \right)^{1/\sum_{i=1}^n w_i} = \exp \left( \frac{\sum_{i=1}^n w_i \ln x_i}{\sum_{i=1}^n w_i} \right) \quad (3.12)$$

where

- $G$  = geometric mean
- $x_i$  = values of samples  $i$
- $n$  = number of samples
- $w_i$  = weight of sample  $i$

### 3.7.3 Harmonic Mean

The harmonic mean of a sequence from Equation (3.9) and (3.10) is the number  $H$  defined by

$$H = \frac{\sum_{i=1}^n w_i}{\sum_{i=1}^n \frac{w_i}{x_i}} \quad (3.13)$$

where

- $H$  = harmonic mean
- $x_i$  = values of samples  $i$
- $n$  = number of samples
- $w$  = weight of samples  $i$

### **3.8 Reservoir Simulation Concept**

Reservoir simulation is a technique to simulate fluid flow in the reservoir. To perform reservoir simulation, a reservoir model is constructed and used to predict reservoir performance under different operating conditions. A reservoir simulation model is a numerical model of the reservoir made up of a large number of cells and uses numerical equations to simulate reservoir performance. The numerical reservoir model is representative of a real geological structure. The equations are solved to examine the reservoir performance in terms of pressure and flow rate. The reservoir is divided into a number of blocks. Basic data are required in each grid block. The wells are positioned within the arrangement of blocks. The required in-flow or out-flow rate is specified as a function of time. The appropriate equations are solved for pressures and saturations for each block as well as the production of each phase for each well.

The basic concept of reservoir simulation is a combination of the conservation of mass, material balance equation, with conservation of momentum, Darcy's Law. These equations along with appropriate constraints, relations, and initial conditions can be solved by approximate numerical techniques to predict the performance of reservoirs under different operating conditions.

In this study, a reservoir simulator was used to simulate the reservoir performance to see the pressure response when a wireline formation test is conducted under different scenarios. Then, a well test interpretation software was used to analyze such pressure response for reservoir parameters

### **3.9 Numerical Solution and Analytical Solution**

Generally, reservoir model is created in the simulator software to represent the reservoir conditions and used to predict the reservoir behavior history. This is a numerical technique used to predict the performance of the reservoir.

Wireline formation test response can be simulated using the simulator. On the other hand, simulated pressure can be interpreted using well test interpretation

techniques. The results from this kind of analysis are estimates of permeability, skin, mobility, etc. This is the analytical analysis technique to obtain reservoir parameters.

In this study, the simulator was used to predict the performance of the reservoir under different conditions and a well test interpretation software is used to obtain the reservoir parameters. However, there is a difference between the mathematical model used in the simulator and flow model used in the well test interpretation software. In the simulator, only a single grid cell around the wellbore was used to represent the probe allowing the only connection between the wellbore and the reservoir while the interpretation software is based on the spherical source solution, which allows fluid to enter a point source. The flow geometries of the two approaches are illustrated in Figure 3.11. Consequently, there is a slightly inconsistency between these two analysis solutions

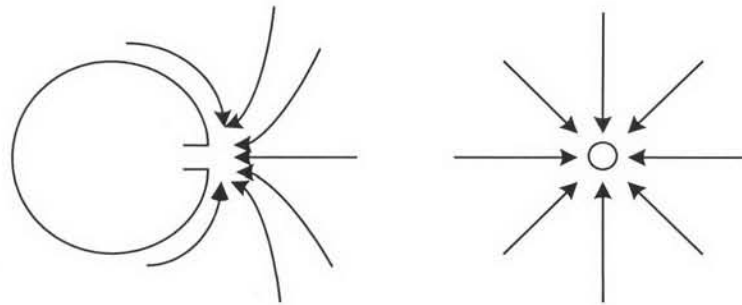


Figure 3.11: Simulation and Well test interpretation software flow geometries for WFT.

### 3.10 Wireline Formation Test Tools

The wireline formation tester was commercially used in 1955 in the Gulf of Mexico, primarily to recover one fluid sample and measure one formation pressure on each trip to the well. Later, the Formation Interval Tester (FIT) was also introduced. In the mid-1970s, Schlumberger's Repeat Formation Testers (RFT) replaced its predecessors FT or FIT, starting in the North Sea, which marked the beginning of a new era in wireline formation testing technology and application. Then, a variety of

wireline testers were available on the market, satisfying the growing need of oil companies in their exploration and development projects. Traditional testers developed in the 1970s and 1980s were very successful in a variety of pressure surveys and applications in single well and reservoir evaluations. In the early 1990s, wireline tester technology took another huge step forward. To provide answers to complex and varied reservoir questions, particularly fluid typing and sampling, Schlumberger designed a new modular tool, Modular Dynamics Formation Tester (MDT), marking a new revolution in wireline formation testing with much enhanced features and capabilities. Then, Baker-Atlas debuted its Reservoir Characterization Instrument (RCI), and in 1999 Halliburton brought Reservoir Description Tool (RDT) to the marketplace.

The current wireline formation testers can be separated into two groups, traditional testers and modern testers. Traditional testers currently still being used in the oil industry, Repeat Formation Tester (RFT), by Schlumberger, Formation Multi-Tester (FMT) by Baker Atlas, Selective Formation Tester (SFT) and Sequential Formation Tester (SFTT) by Halliburton, Repeat Formation Sampler (RFS) by Reeves Wireline and, Formation Tester (FT) by Tucker Wireline, represent the family of traditional wireline testers. Traditional testers have a fixed-volume pretest chamber from 20-cc to 38-cc and cannot perform extended flows for pressure testing or sampling quality control.

For modern wireline testers, several tools were introduced. Schlumberger's MDT, Halliburton's RDT, and Baker Hughes' RCI lead the wireline testing services worldwide. All these three testers have multifunctional features for a broad span of reservoir evaluation applications, from pressures, fluid identification and sampling, to mini-drillstem testing and permeability evaluations. All these three testers are modular tools; each tool string has to be assembled by stacking all required modules before running into the well.

Generally, the modern wireline testers system comprises a number of modules as shown in Figure 3.12. There are four modules making up the basic tool:

- 1) **Electrical module** – This module provides the power to drive all the downhole electronics and a supply for the electro-hydraulic system.



- 2) **Hydraulic power module** – This provides hydraulic power to the probe module.
- 3) **Single probe module** – This module establishes pressure and fluid communication between the tool and the formation. The probe embedded in a circular rubber pad is forced through the mudcake to make a seal with the formation. Two opposing backup pistons on the other side of the tools push the probe against the formation and help maintaining a good seal. After that, the fluid is withdrawn from the formation to the sample chamber. Thus, formation pressure can be measured at the flowrate control.
- 4) **Sample chamber modules** – Any combination of sample chambers can be assembled. A single flowline serves all the chambers.

Others modules can be added to this basic tool:

- 5) **Multisample module** – Each of these modules has several sample chambers. The number of chamber depends on the requirement and/or each company's tools' specification.
- 6) **Pumpout module** – This module pumps formation fluid that has entered the tool out into the borehole.
- 7) **Flow control module** – This module provides pressure drawdown tests with accurately controlled pressure or flowrate.
- 8) **Multiprobe module** – Added to the basic probe module, this creates a tool with three probes, a sink for drawing the fluid and two pressure observation probes. The system is usually configured with the flow control module, drawing fluid through the sink probe to set up a pressure disturbance in the formation. Analysis of transients measured at the two observation probes yields vertical and horizontal permeability estimates and enhances pressure gradient information.
- 9) **Dual-packer module** – This module has two packers. These are inflated by the pumpout module to isolate a zone of borehole from the column of mud. This allows drillstem test (DSTs) and, if the probe module is included, interference tests to be carried out. The packers allow zones to be testes where the probe cannot seal.

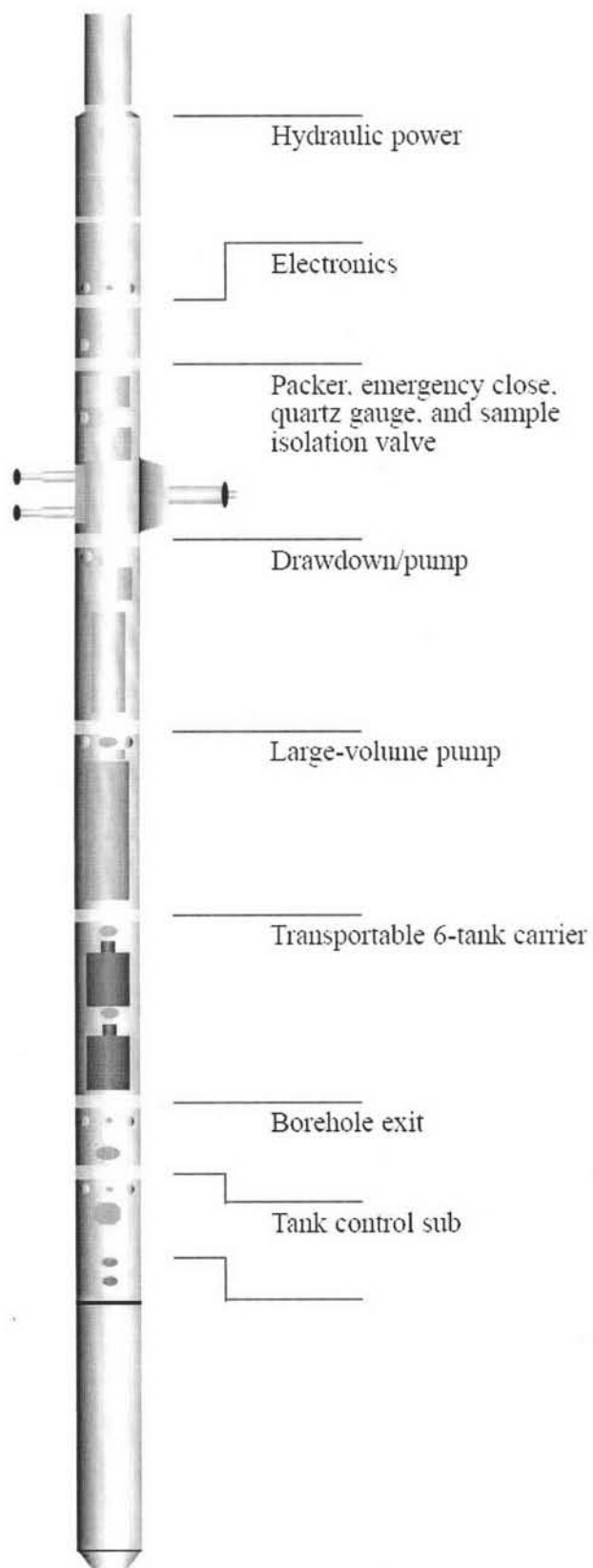


Figure 3.12: Schematic of wireline formation test tool.

This study was emphasizing on the WFT using probe module to perform the test. The analysis uses a spherical source solution model that includes storage, skin, permeability anisotropy, and no-flow boundary and/or constant pressure boundaries.

Assuming infinite top and bottom boundaries, analysis using the probe wireline formation test model yields spherical permeability, fluid compressibility in the test tool, and probe skin factor.

If one or both of the top and bottom boundaries are either no-flow or constant pressure, then the analysis parameters yields spherical permeability, horizontal permeability, vertical permeability, fluid compressibility in the test tool, probe skin factor, distance from the probe to the top boundary, and distance from the probe to the bottom boundary.

### **3.11 Wireline Formation Test and Interpretation Procedure**

To perform wireline formation test, the tool is set in to the borehole. Then, the probe embedded in a circular rubber pad is forced through the mudcake to make a good seal with the formation. Two opposing backup pistons on the other side of the tools push the probe against the formation and help maintaining a good seal. After that, the fluid is withdrawn from the formation to the sample chamber or disposed into the wellbore as schematically showed in Figure 3.13. The pressure gauge records the pressure change during the test. Thus, formation pressure can be measured at the flowrate control.

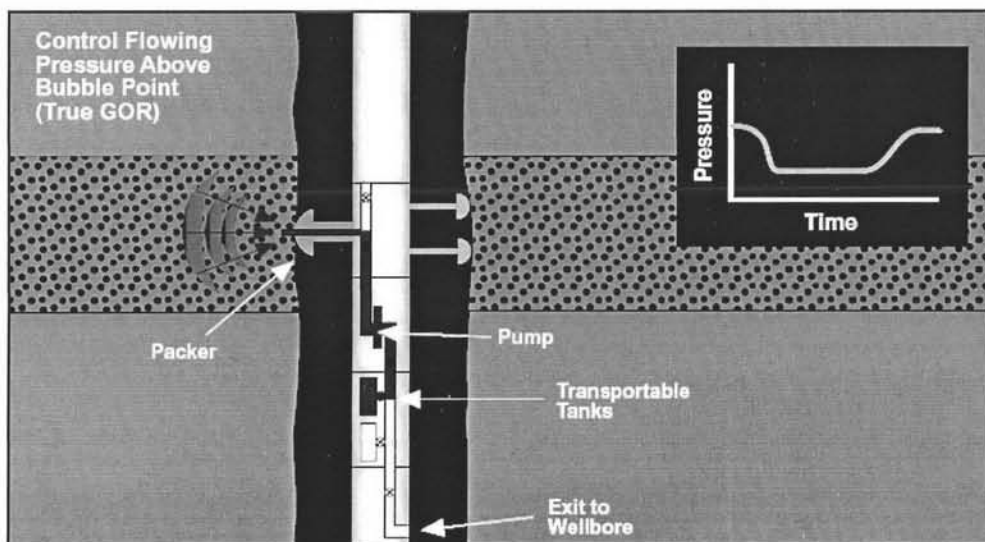


Figure 3.13: Schematic of WFT test.

Figure 3.14 shows pressure and flowrate history of wireline formation test. From point *a* to *b* is wellbore pressure. As the test is continued the tool withdraws the fluid and pressure drops from point *b* to *c*. After the flow is shut, pressure starts to build up to point *d*. From point *d* to *e* is the measured reservoir pressure.

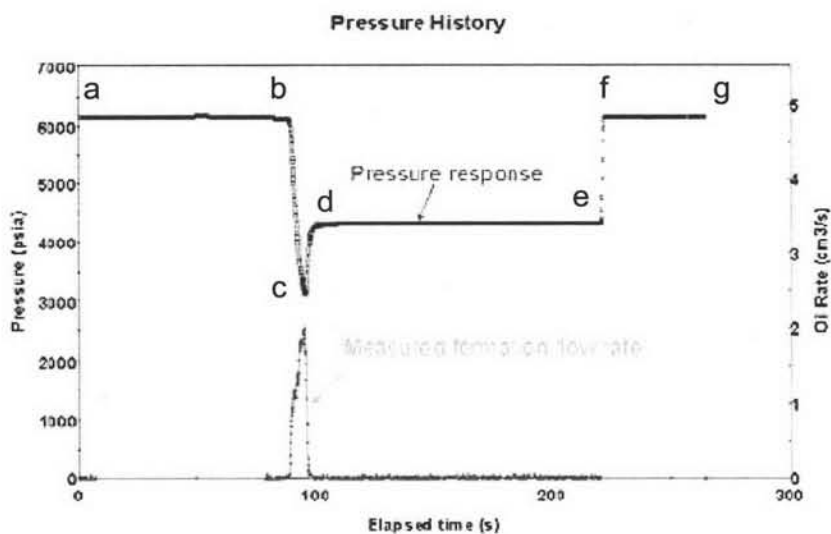


Figure 3.14: Pressure and flowrate history of WFT.

Figure 3.15 shows the pressure history of the repeated test. The first drawdown period is to clean up formation damage and adjust the choke. This period can be called “pretest”. The first buildup provides a first estimate of reservoir pressure such as initial reservoir pressure or mobility. Then, drawdown and buildup are repeated again. It can be seen from the figure that the second and third buildups have the same value of reservoir pressure as the consistent results. As a result, analysis of the pressure response during the second or third buildup reveals the details of the near-wellbore region, formation characteristic such as permeability, and skin factor.

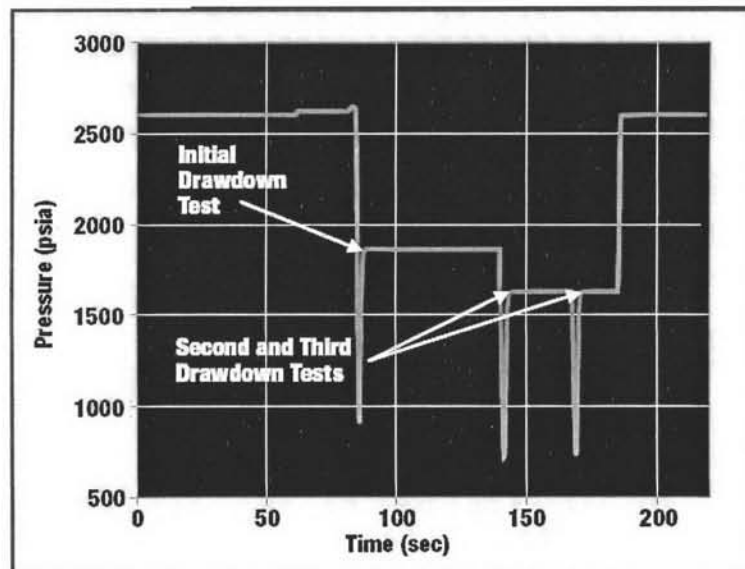


Figure 3.15: Repeated drawdown and buildup tests.

Figure 3.16 shows WFT test and interpretation. As mention before, the first flow period is to clean up the formation. The first build up provides a first estimate of reservoir pressure. Then, repeats drawdown and buildup again. The estimated reservoir parameters are obtained from pressure response during the second buildup. The interpretation can use pressure and flowrate data from both drawdown and buildup period to estimate reservoir parameters. The figure gives example of the test. The diagnostic plot in the figure depicts flow regimes. The radial flow presented in the derivative plot yields the estimated horizontal permeability.

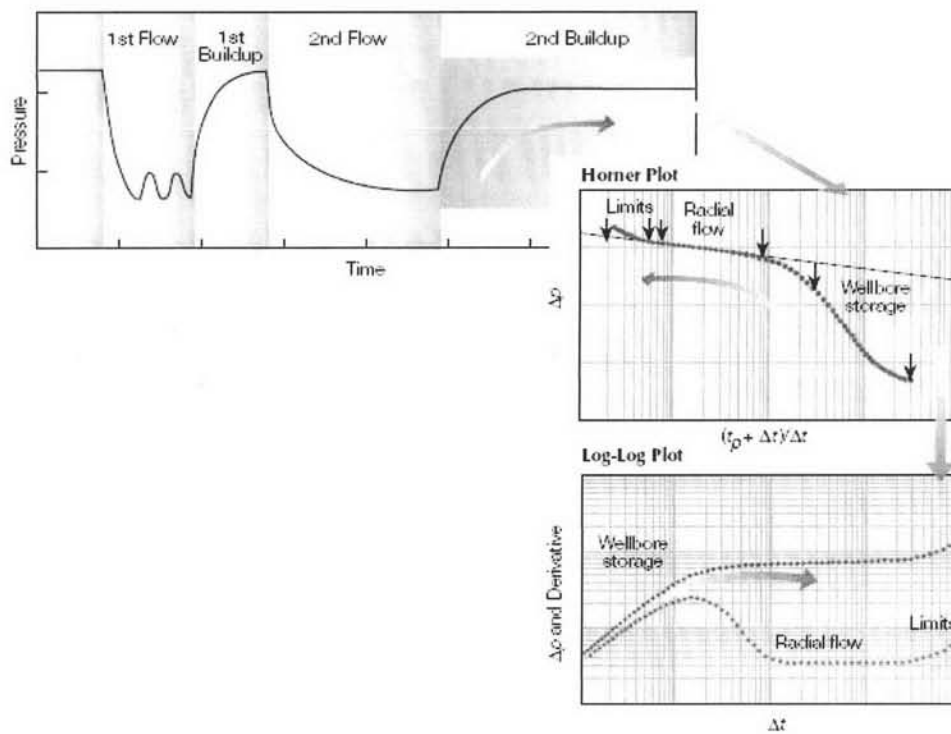


Figure 3.16: Wireline formation test and interpretation.